Hybrid Data-Driven and Model-Based Distribution Network Reconfiguration With Lossless Model Reduction

Nian Liu, *Member, IEEE*, Chenchen Li, *Student Member, IEEE*, Liudong Chen, *Student Member, IEEE*, and Jianhui Wang, *Fellow, IEEE*

***Abstract*—Distribution network reconfiguration is an effective method to face the problem of power fluctuation in the power system. Previous studies have focused on mathematical optimization techniques with complex modeling processes and heuristic algorithms with time-consuming solving processes to obtain the optimal reconfiguration strategy. In this article, a hybrid data-driven and model-based distribution network reconfiguration (HDNR) framework is proposed, where the model-based module includes model reduction and goal-oriented clustering to cluster the identical reconfiguration strategies. Here, the data-driven module is implemented through a long short-term memory network to learn the mapping mechanism between load distribution and optimal reconfiguration strategies. The model-driven module and the data-driven module are coupled through the proposed hierarchical network recovery process, which presents the reconfiguration results layer by layer. Finally, the numerical case study on the IEEE 33-bus, IEEE 119-bus, and IEEE 123-bus network shows the validity of the proposed HDNR framework. It is shown that the solution space is reduced, which contributes to reducing computation time and resources. Moreover, the obtained accuracy of the reconfiguration strategy is higher than most existing research even with limited data samples.**

***Index Terms*—Distribution network reconfiguration (DNR), goal-oriented clustering, hybrid data-driven and model-based, long short-term memory (LSTM), network reduction and recovery.**

Introduction

THE electric load distribution across buses in a distribution network (DN) dynamically changes as the distributed energy resources (DERs) and load patterns vary. The power flow (PF) of the DN changes accordingly [1]. With the more complex operation and control of the DN, power loss reduction has become challenging if the topology of the DN is fixed under a changing load environment [2]. Distribution network reconfiguration (DNR) can change the states of sectionalizing switches and tie switches in the DN. The DNR provides an optimal network structure to realize minimum power losses and achieve better load balancing [3]. In the traditional DN, DNR is not a frequent operation. However, with the application of high-speed switching devices in DN [4], the DNR is developing toward real-time reconfiguration for maintaining the optimal operation condition of DN. Therefore, it is necessary to shorten the computation time and reduce the computation resource of the DNR problem.

Since DNR is a complicated combinatorial optimization problem and the calculation of PF is nonlinear, it is difficult to obtain the optimal reconfiguration strategy of a large-scale DN within a short time. Many studies on this topic can be divided into two categories: 1) mathematical optimization techniques and 2) heuristic algorithms. In the mathematical optimization category, a mixed-integer cone programming model for the DNR problem is proposed [5], which uses exact loss modeling and converges to the global optimal solution. A two-stage optimization model for DNR and a mathematical model for hourly DNR with renewable generation fluctuations are solved based on a similar cone programming model [6], [7]. The Benders decomposition-based approach is also used as an effective method to solve the DNR model with the aim of minimizing the power loss and restricting the voltage volatility [8]. To reduce the computation complexity, the nonlinear term of the network reconfiguration (NR) problem can be linearized by an efficient linearization procedure, then the augmented ε-constraint method is used to solve the NR problem [9]. For considering the uncertainties of DERs, a state-based sequential NR strategy is developed by using a Markov decision process model, which is solved by an approximate dynamic programming approach [10]. However, the complex process of modeling DNR brings about the difficulty of using the cone optimization model, which often leads to a cumbersome simplification process and over-simplified assumptions in the solving process [11].

Various heuristic algorithms are also used to solve the DNR problem. A harmony search algorithm (HSA) is proposed to

Manuscript received October 30, 2020; revised February 28, 2021, May 31, 2021, and August 1, 2021; accepted August 6, 2021. Date of publication August 10, 2021; date of current version February 2, 2022. Paper no. TII-20-4977. *(Corresponding author: Jianhui Wang.)*

Nian Liu, Chenchen Li, and Liudong Chen are with the State Key Laboratory of Alternate Electrical Power System With Renewable Energy Sources, North China Electric Power University, Beijing 102206, China (e-mail: nianliu@ncepu.edu.cn; lichenchen@ncepu.edu.cn; liudong@ncepu.edu.cn).

Jianhui Wang is with the Department of Electrical and Computer Engineering, Southern Methodist University, Dallas, TX 75205 USA (e-mail: jianhui@smu.edu).

Color versions of one or more figures in this article are available at https://doi.org/10.1109/TII.2021.3103934.

Digital Object Identifier 10.1109/TII.2021.3103934

obtain the optimal reconfiguration strategy [12], [13]. Furthermore, a segmented-time reconfiguration problem of DN is solved by a hybrid particle swarm optimization (PSO) method [14]. To improve the accuracy of the heuristic algorithm, a switch opening and exchange (SOE) method for the DNR is proposed [15], which adopts a combination of the sequential switch opening method and the branch exchanging method [16]. Moreover, crossover and mutation are introduced in the heuristic algorithm to speed up the process of obtaining an optimal strategy [17]. For example, an improved tabu search algorithm is presented to solve the loss-minimization reconfiguration in large-scale distribution systems [18]. A genetic algorithm (GA) is applied to minimize the day-ahead total operation costs of distributed generations (DGs) and responsive load, and obtain the optimal topology for the DN [19]. The random-key generic algorithm is used to minimize resistive losses, the risk of violating state estimator accuracy, and the number of meters installed in the DN [20]. A multiobjective molecular differential evolution algorithm is designed to solve the NR model with the objectives of minimizing three-phase unbalanced factors and the number of switching times [21]. To improve the population diversity and search ability of evolutionary algorithm in the solving process of DNR problem, a hybrid evolutionary algorithm combing shuffled frog leaping algorithm and particle swarm optimization method is proposed to obtain the optimal NR strategy [22]. Although these heuristic methods perform well in specified scenarios, the process of converging to an optimal strategy is slow and time-consuming for a large-scale DN.

Data-driven methods, which include machine learning with many kinds of neural networks, are applied to the DN. By learning the underlying mapping mechanism between the input and output of the neural network, a large amount of historical data is effectively used to solve these problems. For example, reactive power optimization considering uncertainty in DN [23], distribution system state estimation [24], parameter and topology joint estimation in DN [25], topology identification of low voltage DN [26], and event detection for the distribution system [27] are investigated. The performance and dimension of the neural network are affected by the amount of data and the type of data. Generally, since the switch actions are determined by the load distribution across buses on the network, the mapping mechanism between load data and the optimal reconfiguration strategy can be approximated by a neural network, which can avoid the complex modeling process and long computation time of traditional methods.

However, few studies focus on the data-driven method in the DNR problem, most of them consider the real-time data measurement for DNR [28], or use collected load data for reinforcement learning [29]. The mapping mechanism has also been studied in [30] through the data-driven method. The focus is on the real-time reconfiguration, while the solution space, computation dimension, required data, and learning accuracy are still the open question. Therefore, although the application of the data-driven method in the DNR problem has been explored, three challenges about the requirements of large amounts of data and the high computation dimension have still existed: 1) dimension reduction of the DN by reducing the number of buses, which can avoid the complex learning process resulting from the large solution space of the DNR problem; (2) data labeling for the optimal reconfiguration strategy learning, which is due to the difficulty of directly applying a large amount of load data to the data-driven DNR problem; and 3) accurate optimal reconfiguration according to the reduced network.

Therefore, to address the aforementioned problems, a hybrid data-driven and model-based distribution network reconfiguration (HDNR) framework is proposed to reduce the solution space and realize the fast reconfiguration. The work here has the potential to open new research opportunities for the complex network related problems in terms of network reduction, processing, and recovery. The contributions are as follows:

1) An HDNR framework is created with the DN model reduction and hierarchical recovery process. In the framework, a goal-oriented clustering model for reconfiguration strategies is proposed, while the data-driven method is designed for the mapping mechanism. Besides, the data-driven and model-driven methods are coupled by the hierarchical recovery process.
2) The model-driven method based on the model reduction and goal-oriented clustering model is proposed for obtaining the data sample of the learning network. The model reduction is proposed to reduce the number of buses in the DN for the smaller solution space of the DNR problem and input matrix of the learning network. Furthermore, the goal-oriented clustering model for reconfiguration is provided to build the data class label for the learning network.
3) The data-driven method is realized with the help of the long short-term memory (LSTM) neural network. Hierarchical databases are built by combining the data-driven method, the proposed recovery process, and the model-driven method. Each database in one layer corresponds to one specific recovery network and the corresponding solution is gradually approaching the precise solution. Then, the optimal reconfiguration strategy can be obtained by utilizing both the model-driven and data-driven methods.

II. HDNR Framework

The states of multiple switches should be decided simultaneously in the DNR. The mentioned fact results in a complex large-scale combinational optimization problem, and brings about great challenges to efficiently decide the optimal reconfiguration strategy. By reducing the solution space of switch combinations and using the data samples to implement a data-driven method, the proposed HDNR framework improves the efficiency of obtaining a reconfiguration strategy. The three aforementioned challenges of the DNR problem can be solved by the HDNR framework shown in Fig. 1.

First, a model reduction is provided to reduce the neural network input dimension through aggregating multiple buses, reducing the number of buses, switches, and corresponding switch combinations in the DN. Second, a goal-oriented clustering model is proposed to obtain the cluster and data class label of an

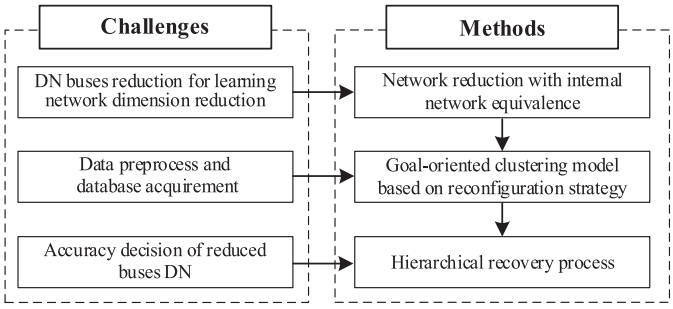

Fig. 1. HDNR framework.

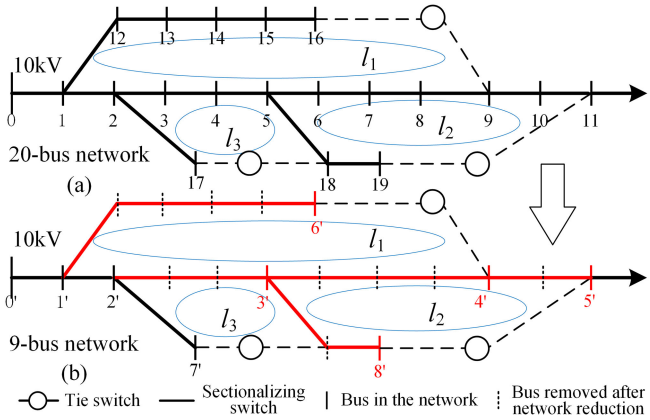

Fig. 2. Network reduction process.

optimal reconfiguration strategy. The goal-oriented clustering model groups the data samples with the same reconfiguration strategy. According to these clusters, the data-driven learning method can obtain the mapping mechanism between load distribution and the optimal reconfiguration strategy, and realize fast decision-making. Finally, a hierarchical recovery process is used to implement lossless decision-making with fewer buses in the DN. The process is nested in the goal-oriented clustering model and learning method to recover the switches from the reduced network hierarchically. It is noted that the HDNR framework possesses a lossless decision-making process. The complex reconfiguration model is reduced to a simple one based on the HDNR framework, and the optimal switching strategies obtained through the HDNR framework are the same as the original network.

III. Distribution Network Reduction

A DN can be regarded as a directed graph composed of buses and branches $G = (V, E, A)$, in which V is a finite set with N buses, E is the set of edges, A is the adjacent matrix of G, and the degree of a bus used to express the number of connected buses is defined as D [31], [32]. The network structure is shown in Fig. 2(a). Each branch has a sectionalizing switch or tie switch, and each bus in DN is connected by a branch with a switch. One tie switch can form a loop with other sectionalizing switches. In the initial state of the network, as shown in Fig. 2(a), the tie switch will be open to satisfy the radial structure requirement of the DN.

Definition 1: In a DN defined as G, network reduction is conducted in the way that an equivalent bus is a combination of sequentially connected buses with $D = 2$, and the corresponding equivalent switch is also an aggregation of the switches between buses with $D = 2$. At the same time, the network power losses should keep unchanged.

According to Definition 1, buses (3, 4, 5), (6, 7, 8, 9), (10, 11), (12, 13, 14, 15, 16), and (18, 19) in the 20-bus network in Fig. 2(a) can be aggregated into one bus, respectively, resulting in the network in Fig. 2(b). The bus and branch in red is the aggregated (equivalent) bus and equivalent branch. For example, bus 3′ is the equivalent bus of buses (3, 4, 5) and branch 2′–3′ is the equivalent branch of branches (2–3, 3–4, 4–5).

The equivalent nodal load and branch impedance of the network reduction process can be obtained by external network equivalence [33]. However, the external network equivalence is complex, dynamic, and time-consuming. The topology of the external network and the states of the network switches change constantly in the DNR. Therefore, it is difficult to use the external network equivalence in the DNR problem. Theorem 1 below is proposed to provide an alternative method for obtaining the parameters of the reduced network.

Theorem 1: The equivalent bus is a combination of the sequentially connected buses with $D = 2$ under the constraints of constant branch power loss, and the branch parameters and

$$\begin{cases} X' = X_{01} + X_{12} + \cdots + X_{(n-1)n} \\ Q' = \sqrt{\dfrac{(Q_1+Q_2+\cdots+Q_n)^2 X_{01}}{(X_{01}+X_{12}+\cdots+X_{(n-1)n})} + \dfrac{(Q_2+\cdots+Q_n)^2 X_{12}}{(X_{01}+X_{12}+\cdots+X_{(n-1)n})} + \cdots + \dfrac{{Q_n}^2 X_{(n-1)n}}{(X_{01}+X_{12}+\cdots+X_{(n-1)n})}} \end{cases} \tag{1}$$

$$\begin{cases} R' = R_{01} + R_{12} + \cdots + R_{(n-1)n} \\ P' = \sqrt{\dfrac{(P_1+P_2+\cdots+P_n)^2 R_{01}}{(R_{01}+R_{12}+\cdots+R_{(n-1)n})} + \dfrac{(P_2+\cdots+P_n)^2 R_{12}}{(R_{01}+R_{12}+\cdots+R_{(n-1)n})} + \cdots + \dfrac{{P_n}^2 R_{(n-1)n}}{(R_{01}+R_{12}+\cdots+R_{(n-1)n})}} \end{cases} \tag{2}$$

$$\begin{aligned} \Delta P &= \Delta P_2 + \ldots + \Delta P_n + \Delta P_{n+1} \\ &= \frac{(R_{12}+R_{23}+\ldots+R_{n(n+1)})}{U^2} \left(\sqrt{\frac{(P_2+P_S+\ldots+P_{n+1})^2 R_{12}}{R_{12}+R_{23}+\ldots+R_{n(n+1)}} + \frac{(P_S+\ldots+P_{n+1})^2 R_{23}}{R_{12}+R_{23}+\ldots+R_{n(n+1)}} + \ldots + \frac{{P_{n+1}}^2 R_{n(n+1)}}{(R_{12}+R_{23}+\ldots+R_{n(n+1)})}} \right)^2 = \frac{R'}{U^2} P'^2 \end{aligned} \tag{3a}$$

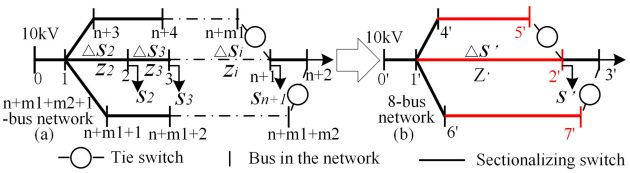

Fig. 3. Equivalence process.

nodal load should meet (1) and (2), Both are shown at the bottom of the previous page,

$$\Delta P_n = \frac{P_n^{\,2}}{U_n^2} R_{(n-1)n} \tag{3b}$$

where R', X', P', and Q' are the resistance, reactance, active power, and reactive power of one branch, respectively; $R_{(n-1)n}$ and $X_{(n-1)n}$ are the impedance of branch $(n-1)-n$, P_n and Q_n are, respectively, the active power and reactive power of the bus n.

Proof: Fig. 3 shows a general network with $(n + m1 + m2)$ number of buses. The equivalence process of the branches $1 - (n + 1)$, $(n + 3) - (n + m1)$ and $(n+m\ 1 + 1) - (n + m\ 1 + m2)$ is described in this figure. The active power loss of the branch $1 - (n + 1)$ in Fig. 3(a) can be calculated and expressed in (3a) shown at the bottom of the previous page. Here, we assume that the nodal voltage is the same [3], [34].

The equal sign in (3b) is satisfied due to the small reactive power and power loss of a single branch, and the equal sign in (3a) is satisfied because the deviation of nodal voltages is small under normal operation. n buses can be equivalent to one bus based on (3a) and (3b), while the value of power losses caused by the nodal power and branch impedance remains unchanged. According to (3a) and (3b), (2) can be obtained by recursion, which shows the equivalent active power and resistance. Similarly, when the reactive power losses remain unchanged, the mathematical expression [i.e., (1)] of equivalent reactive power and reactance can be obtained.

Specifically, the influence of null injection bus and weakly mottled nets on the model reduction is also analyzed. For the null injection bus, the power is zero, and there is no influence on the model reduction. As the branches $1-(n + 1)$ shown in Fig. 3, suppose the bus n is a null injection bus, the P_n in the model reduction (3) is changed to 0. The calculation method of equivalent active power P' of the model reduction is similar to the positive active power. Therefore, the null injection bus does not affect the network reduction process and the calculation of equivalent nodal load.

For the weakly mottled nets, suppose the branch 2–3 in Fig. 3 has a large resistance R_{23}, the model reduction is expressed as

$$\Delta P = \frac{(R_{23})}{U^2}\left(\sqrt{\frac{(P_3+\cdots+P_{n+1})^2 R_{23}}{(R_{23})}}\right)^2 = \frac{R'}{U^2}P'^2. \tag{4}$$

The resistance of other branches can be set as 0 when compared with the R_{23}, so $R_{12} + R_{23} + \cdots + R_{n(n+1)} = R_{23}$. The equivalent power P' can also be calculated by the model reduction. Therefore, the weakly mottled nets (which have large branch resistance) can also be reduced by the model reduction and do not influence the network reduction process.

According to Theorem 1, the model reduction is only affected by the nodal load and the branch impedance that are directly associated with the reduced branch. The number of network buses (i.e., the scale of the network) may not affect the effectiveness of the model reduction. The model reduction can be regarded as an internal network equivalence and remain unchanged when the external network changes. As a result, the problem that network equivalence changes with the structure of external network is avoided, which reduces the computational complexity, and shortens the computation time. It is noted that the variation of DGs and loads have no influence on the model reduction because the model reduction only reduces the network structure for the DNR problem. The variation of DGs and flexible loads during the reconfiguration process remain. To deal with the variation, the reconfiguration model should be built with the consideration of variation.

As the optimization goal of the reconfiguration problem is to get minimal power losses, for the bus with $D \leq 2$, the model reduction keeps parameters of the reduced network and the original network equivalence in terms of the power loss, so that it keeps the optimality at the theoretical level. However, for the bus with $D > 2$, the value of power losses may change a little after the network reduction. Because the power losses are determined by the impedance of all branches and the load of all buses. Therefore, some correction needs to be introduced to address this issue and obtain the optimal reconfiguration strategies. In Section IV, a specific correction method for DNR problem with meshed networks is introduced in detail.

IV. Goal-Oriented Clustering for Reconfiguration

In general, directly solving the DNR problem is not an easy task because of its complex combinatorial nature. A goal-oriented clustering model is proposed here to reduce the problem size and computational complexity. The goal of clustering is to group optimal reconfiguration strategies under the objective of minimizing power losses. The clustering process basically solves the following problem [35]:

$$\Gamma_m \in \arg\min g\left(\boldsymbol{K}_{\boldsymbol{S}}^*\left(\Gamma_m\left(\boldsymbol{K}_{\boldsymbol{Sm}}^*\right)\right), \boldsymbol{K}_{\boldsymbol{Sm}}^*\right), 1 \leq m \leq M \tag{5}$$

where m denotes the clustered index, the number of clusters is M, $\boldsymbol{K}_{\boldsymbol{Sm}}^*$ is the optimal reconfiguration strategy in cluster m, Γ_m minimizes the sum of Euclidean distance between the optimal reconfiguration strategy $\boldsymbol{K}_{\boldsymbol{Sm}}^*$ and its representative $\Gamma_m(\boldsymbol{K}_{\boldsymbol{Sm}}^*)$, and $g(\cdot)$ is the clustering objective function.

The goal-oriented clustering results can be expressed as follows:

$$C_m^* = \left\{\boldsymbol{K}_{\boldsymbol{Sm}}^* | g\left(\boldsymbol{K}_{\boldsymbol{Sm}}^*, \boldsymbol{K}_{\boldsymbol{S-m}}\right) \leq g\left(\boldsymbol{K}_{\boldsymbol{Sm}}, \boldsymbol{K}_{\boldsymbol{S-m}}\right), 1 \leq m \leq M\right\} \tag{6}$$

where C_m^* is the clustering results and $\boldsymbol{K}_{\boldsymbol{S-m}}$ denotes the other reconfiguration strategies, except cluster m.

Since the clustering model is based on the DNR problem, it may inevitably need to calculate the PF of the system. As every single branch has individual power loss and switching actions may also cause certain loss. The switching action means changing the switches' state when conducting the DNR, i.e., the open state change to closed state and closed state change to open state. The switches have a specific life span, changing the state may reduce their life span [28]. To make the life span cost of the switch be added to the power losses from PF, the reduction of switches' life span is regarded as a kind of power loss in the DNR problem. The power losses of the entire system can be given as

$$\Delta P = \sum_{i,j\in N} P_{\text{loss}}(i,j) + P_{\text{switch}} = \sum_{i,j\in N} R_{ij}\frac{P_{fj}^2+Q_{fj}^2}{U_j^2} + \sum_k GC_{\text{sw}} \tag{7}$$

where *ij* is the branch between bus *i* and *j*, the number of buses in DN is *N*, R_{ij} and X_{ij} are the resistance and reactance of branch *ij*, P_{fj} and Q_{fj} is the active and reactive PF out of the bus *j*, and can be calculated based on the nodal load. U_j is the voltage at the bus *j* and *G* is the number of switching actions. C_{sw} is the power loss from one action of each switch.

The reconfiguration problem is formulated as a function of the number of switching operations and bus voltage. The constraints of the DNR problem consist of the power line transmission capacity, bus voltage limit, power balance, and radial structure of DN [5], which can be expressed as follows:

$$\min f(\boldsymbol{K}_{\mathbf{S}}, G, U_j) = \sum_{i,j\in N} k_{ij}R_{ij}\frac{P_{fj}^2+Q_{fj}^2}{U_j^2} + \sum_k GC_{\text{sw}} \tag{8}$$

$$\text{s.t. } P_{\text{cap}}^- < P_{ij} < P_{\text{cap}}^+ \tag{9}$$

$$U_{j\_\min} \le U_j \le U_{j\_\max} \tag{10}$$

$$\Delta P + \sum_{i\in N}(P_{Li}) = \sum_{i\in N} P_{Gi} \tag{11}$$

$$\sum_{i,j\in N} k_{ij} = N-1 \tag{12}$$

$$\alpha_{ij} + \alpha_{ji} = k_{ij} \tag{13}$$

$$\sum_{j\notin N_{\text{Sub}}} \alpha_{ij} = 1 \tag{14}$$

$$\sum_{j\in N_{\text{Sub}}} \alpha_{ij} = 0 \tag{15}$$

where k_{ij} is the state of the switch in the line *i*–*j* (if the state is open, $k_{ij} = 0$, otherwise, $k_{ij} = 1$), $\boldsymbol{K}_{\mathbf{S}}$ is the set of k_{ij}, P_{cap}^- and P_{cap}^+ are the lower and upper bound of power line transmission capacity. P_{ij} is the transmission power of power line *i*-*j*. $U_{j\_\min}$, $U_{j\_\max}$ are the lower and upper bound of nodal voltage. P_{Li} and P_{Gi} are the load power and generator power, respectively. α_{ij} is a binary variable indicating if the bus *j* is the parent of the bus *i*, and N_{Sub} is the set of substation buses. Equations (9)–(11) are, respectively, the constraints of the power line transmission capacity, nodal voltage limit, and power balance. Equations (12)–(15) are the radial structure constraints: (12) shows the network topology needs to be a tree, (13) guarantees that only one of two buses can be the parent bus of the other one for a connected branch, and (14) indicates that each bus can have at most one parent bus. Equation (15) shows that the starting bus cannot be the parent bus for a branch connected to the substation bus.

DNR is a complex combinatorial optimization problem because of the multiple DN loops. Based on graph theory, the global optimal solution of the DNR problem can be solved by HSA with some improvement [36], and the harmony matrix (HM) is updated to an initial HM and surplus HM with both HMs satisfying the radial topology structure of the DN. The network topology can then be obtained from the state of switches.

The existence of the $D > 2$ buses results in power losses in the reduced network deviating from the original network in terms of series branches. Although the DN is regulated to operate in the radial structure, the DN is designed in the form of a closed-loop to improve operational flexibility and power supply reliability. Moreover, the tie switch is used to connect two different series branches and keep open in the initial state of the network. Therefore, the tie switch and the sectionalizing switch corresponding to the $D > 2$ bus in a loop are on different series branches. For example, in the loop l_1 of Fig. 2(b), the tie switch 4′–6′ and the sectionalizing switch 3′–4′ corresponding to the bus 4′ are on series branches 1′–6′ and 1′–4′, respectively. The change of power loss in a series branch where the $D > 2$ bus is located may lead to a misjudgment of the state of sectionalizing switches and tie switches. Therefore, the correction method shown in (16) is proposed to achieve the optimal results. The correction method [i.e., (16)] means comparing the power losses under, respectively, open sectionalizing switches and tie switches scenarios, then selecting the minimum one as the optimal strategy. The optimization problem can be expressed as

$$\min\left(f\left(\boldsymbol{K}_{\boldsymbol{Sl}}^{\boldsymbol{B}}, G^*, U_j^*\right), f\left(\boldsymbol{K}_{\boldsymbol{Sl}}^{\boldsymbol{T}}, G^*, U_j^*\right)\right) \tag{16}$$

where $\boldsymbol{K}_{\boldsymbol{Sl}}^{\boldsymbol{B}}$ is the sectionalizing switch in loop *l* and $\boldsymbol{K}_{\boldsymbol{Sl}}^{\boldsymbol{T}}$ is the tie switch in loop *l*.

The optimal reconfiguration strategy $\boldsymbol{K}_{\mathbf{S}}^*$ for the clustering model can be acquired by solving the problem (8)–(15) with the correction method, and the optimal strategy satisfies the following inequation:

$$f\left(\boldsymbol{K}_{\mathbf{S}}^*, G^*, U_j^*\right) \le f\left(\boldsymbol{K}_{\mathbf{S}}, G, U_j\right). \tag{17}$$

V. Reconfiguration Decision-Making With Data-Based Learning and Recovery Process

A. Data-Driven Learning Method for Reconfiguration Database

Based on the goal-oriented clustering results, the load distribution with the same optimal reconfiguration strategies $\boldsymbol{K}_{\boldsymbol{Sm}}^*$

is clustered into one cluster and marked with one kind of class label for data-driven learning. The class label can be expressed as

$$L_m = \{l_m | \boldsymbol{K}_1^* = \boldsymbol{K}_2^* = \ldots = \boldsymbol{K}_{\boldsymbol{Sm}}^*, 1 \le m \le M\} \quad (18)$$

where L_m is the class label, and $\boldsymbol{K}_1^*$ and $\boldsymbol{K}_2^*$ are the optimal reconfiguration strategy of different load distributions.

According to the class label and corresponding reconfiguration strategy, the data-driven learning method is used to obtain the mapping mechanism between load distribution and optimal reconfiguration strategies. The LSTM model has advantages in handling problems that have long-term dependencies (e.g., the load of the current hour is related to the load of the next hour). LSTM network is composed of an input layer, a hidden layer, and an output layer. In the hidden layer, the forget gate mechanism can help the LSTM network process the series input data. A memory cell is used in the blocks in the hidden layer, which can build the relationship between the current node and the previous node, the coupled input information can be transmitted and kept through the memory cell [37]. Therefore, the LSTM network is used to build the mapping mechanism for the reconfiguration problem.

The features of the LSTM network are composed of the optimal reconfiguration results, including two parts: network structure and nodal power injections. This information forms a feature matrix, which is expressed as

$$Pi \in N \times 2 \quad (19)$$

where N is the number of buses, 2 refers to the active power and reactive power of each bus calculated by the reconfiguration model. Both buses and their power are corresponding to their network label. Since each element in the matrix corresponds to the network of the distribution system, each feature affects the classification accuracy of reconfiguration strategy clustering.

The output of the LSTM network is the labeling of the clustering results. The features are used as the input and the corresponding class label is used as the output of the LSTM network. The three gates (forget gate, input gate, and output gate) in an LSTM cell helps to form the relation between input and output, as well as minimize the learning error [37]:

$$J = \frac{1}{a} \sum_{i=1}^{a} \sum_{j=1}^{M} y_j^{(i)} \log \hat{y}_j^{(i)} \quad (20)$$

where a is the number of samples, $y_j^{(i)}$ and $\hat{y}_j^{(i)}$ are the true and predicted class label, respectively.

Therefore, through taking load distribution as the input and the corresponding class label as the output, the mapping mechanism between the load distribution and the resultant reconfiguration strategies is achieved. This mapping mechanism can conveniently generate reconfiguration strategies based on the load distribution given to the LSTM network.

The load distribution presents a certain similarity because of the inertia of the users' energy consumption behavior. Besides, the number of switches is reduced due to the model reduction. Considering the above two factors, there may be fewer categories of optimal reconfiguration strategies and LSTM's outputs. Therefore, a small number of samples can obtain a high accuracy when training the LSTM network.

B. Reconfiguration Strategy With Network Recovery

To obtain the optimal reconfiguration strategy of the original network, a recovery process should be conducted based on the reduced network and its optimal switch strategy. The details of the network recovery process are presented as follows:

If the switches in the equivalent branch are open, the branch i–j should be separated into two branches: branches i-i' and i'-j. The conjunction point of this branch can be determined by the following principles:

1) if there are $2k-1$ sectionalizing switches in the original network corresponding to the equivalent branch i–j, then the branch i-i' should have $k-1$ sectionalizing switches, and the branch i'-j should have k sectionalizing switches;
2) if there are $2k$ sectionalizing switches in the original network corresponding to the equivalent branch i–j, then branch i-i' should have k sectionalizing switches, and the branch i'-j should have k sectionalizing switches.

The parameters of the branches i-i', i'-j, and the real/reactive power of bus i' can be determined by Theorem 1. Through this recovery process, the reduced network is recovered layer by layer until the stop criterion is satisfied, where the stop criterion means the number of switches with an undetermined state is no more than N_0 in each loop. Besides, N_0 is flexibly determined by the number of samples and the current recovery network.

The network recovery takes a hierarchical approach. This process is expressed in Fig. 4. $\boldsymbol{K_o}$ is the optimal reconfiguration strategy of each layer. $\boldsymbol{k_t}, t \in \{1, 2, 3\}$ is the possible state combination of every switch in the loop l_t. k_t is the switch whose state has been determined in the loop l_t. The layered process is determined by the switches' states under the optimal reconfiguration strategies of the reduced network. In Fig. 4, the reconfiguration strategies of the reduced network are $\boldsymbol{K}_{021}$ and $\boldsymbol{K}_{022}$, where the network structure is different from the original network to a great extent. To recover the original network and according to the reduced network and the strategy $\boldsymbol{K}_{022}$, the branches 3′–4′ and 2′–8′ in the network $\boldsymbol{K}_{022}$ are separated to the branches 3′-a_2, a_2-4′ and 2′-a_3, a_3-8′, respectively. There are three different reconfiguration strategies of the reduced network $\boldsymbol{K}_{022}$: $\boldsymbol{K}_{031}$, $\boldsymbol{K}_{032}$, and $\boldsymbol{K}_{033}$. Each network needs to be continuously recovered. The branch 2′-a_3 is separated into the branches 2′-a_{31} and a_{31}-a_3 in $\boldsymbol{K}_{031}$. Then, if the number of switch whose states have not been decided in the current network is not more than N_0, the recovery process is terminated.

If the last layer is still not the original network, there are at most N_0 switches that need to be judged in each loop, and the solution space is greatly reduced compared with the original network. Therefore, the reconfiguration model of (8)–(15) is modified to a simple combinatorial selection problem, and can be solved by a simple enumeration method in a small solution space, which is expressed as follows:

$$\min\{A, B \ldots | A = f(\boldsymbol{k}1^{\boldsymbol{m}}), B = f(\boldsymbol{k}2^{\boldsymbol{m}}), \ldots\} \quad (21)$$

$$s.t. \text{ Eqs. } (9-11) \quad (22)$$

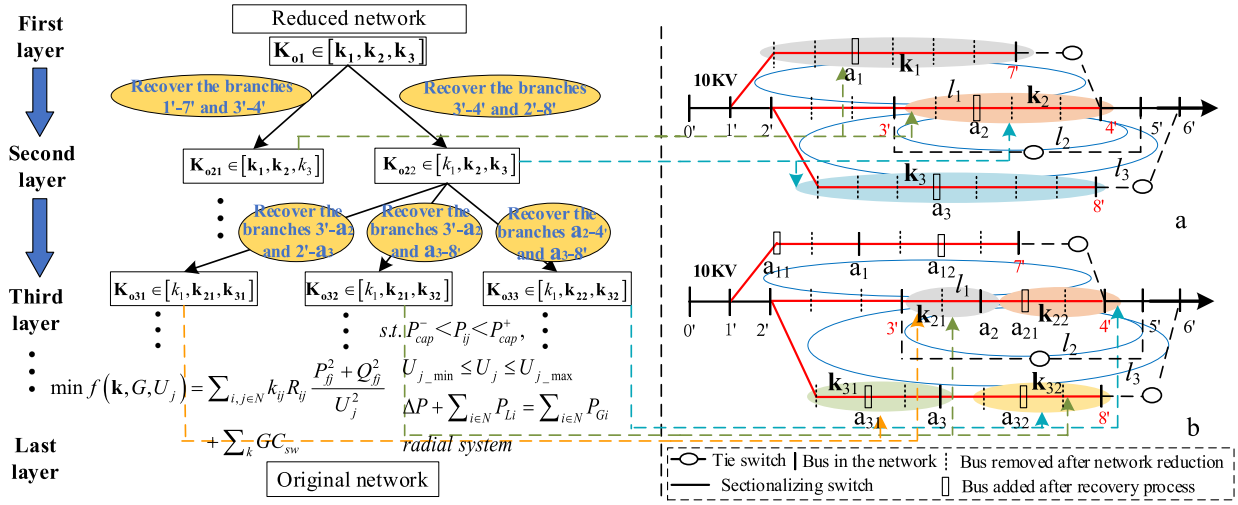

Fig. 4. Layering recovery process of reconfiguration.

where $\boldsymbol{k}1^{m}$ and $\boldsymbol{k}2^{m}$ are the switches set in the cluster m of the last layer.

For the DNR problem in a specific network, through the hierarchical recovery process, the solution space is greatly reduced. Therefore, the computation time is vastly shortened, and computation resources are saved. It is noted that the complexity of the proposed method is depended on the number of loops (i.e., tie switch) and sectionalizing switch in the network.

In the HDNR framework, through building the mathematical model for the model-driven method, the samples can be generated and the learning network for the data-driven method is built, then the DNR is implemented in a less solution space, fast realization, and better results. The LSTM network used in the solving process serves as the data-driven method and is implemented with the designed hierarchically recovery process, which is the basis for the foundation of reconfiguration databases. The databases then help the proposed HDNR framework realize the fast reconfiguration. A pseudocode of the HDNR framework for DNR is as follows.

HDNR framework.

1. Input network structure and load information.
2. Reduce the network based on (1) and (2).
3. Cluster the sample with the goal of the same optimal reconfiguration strategy in (5)–(17).
4. Build the database based on the LSTM network.
5. Recovery process

While num$> N_0$ (*num* is the number of switch undetermined in current recovery network)

do

Step 3 for a recovered network.

Step 4 for a recovered network.

Build the recovered network based on the results of Step 4.

End while

6. Select the optimal reconfiguration strategy in (21)–(22).

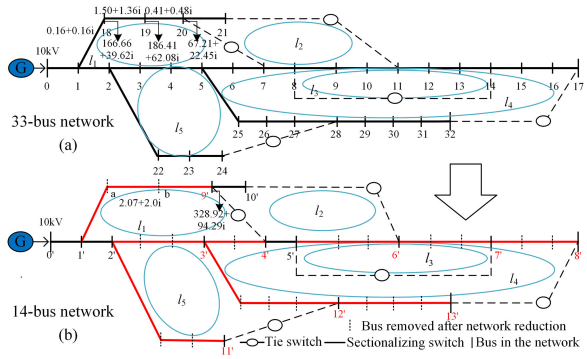

Fig. 5. Reduction process from 33-bus network to 14-bus network.

VI. Case Study

A. Data

The IEEE 33-bus network is used as the network topology in this article to verify the proposed model, which includes 59 users, and the data of the system is taken from an industrial park in Henan Province, China with 665 days. Fig. 5(a) shows the topology of the system that is composed of five loops. In the network, each bus is connected to a distribution transformer that connects n users, which consists of residents, commercial buildings, and factories. Each user is equipped with a user energy management system to collect data, store data, and conduct calculations. The DNR is performed by the utility grid according to the existing environment of the power system. Besides, the proposed model is also performed in the IEEE 119-bus and IEEE 123-bus test networks.

B. Results of Network Reduction

The IEEE 33-bus network can be reduced to a 14-bus network based on the model reduction. Fig. 5(b) shows the 14-bus network, where the red branch is an equivalent branch of multiple branches in the original network; for example, branch 1′–9′ comes from the three branches (1′-a, a-b, b-9′). Moreover,

TABLE I
RECONFIGURATION STRATEGY OF THE FIRST LAYER

Cluster label	Loop 1	Loop 2	Loop 3	Loop 4	Loop 5
1	3'-4'	5'-6'	6'-7'	7'-8'	3'-12'
2	4'-9'	5'-6'	6'-7'	7'-8'	3'-12'

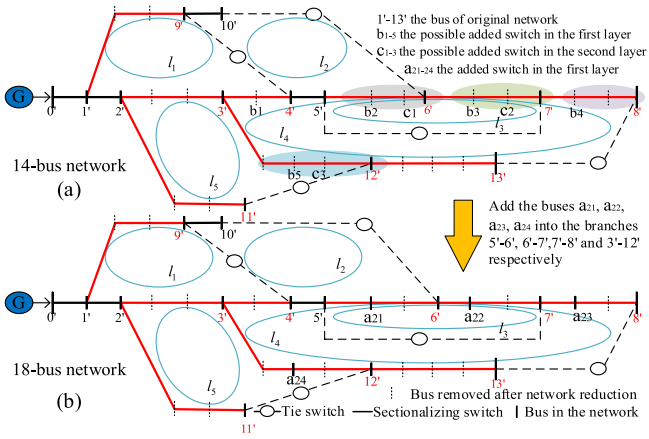

Fig. 6. Recovery process from 14-bus network to 18-bus network.

TABLE II
RECONFIGURATION STRATEGY OF THE SECOND LAYER

Network	Loop 1	Loop 2	Loop 3	Loop 4	Loop 5
19-bus	b_1-4'	5'-b_2	b_3-7'	b_4-8'	b_5-12'
	b_1-4'	b_2-6'	b_3-7'	b_4-8'	b_5-12'
	4'-9'	5'-b_2	b_3-7'	b_4-8'	b_5-12'
18-bus	3'-4'	b_2-6'	b_3-7'	7'-b_4	b_5-12'
	4'-9'	5'-b_2	b_3-7'	7'-b_4	b_5-12'
	4'-9'	5'-b_2	b_3-7'	b_4-8'	b_5-12'

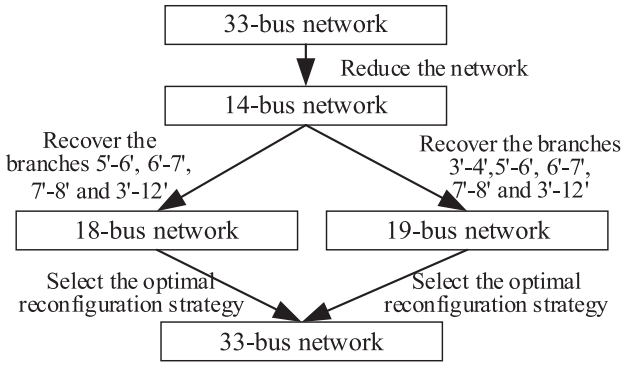

Fig. 7. Changing process of network.

three buses (a, b, 9′) are merged into one equivalent bus 9′. The impedance of each branch and the complex power of each bus are also shown in Fig. 5(b). According to (1) and (2), the impedance of equivalent branch 1′–9′ is $2.07 + 2.0i$, and the complex power of the equivalent bus 9′ is $328.92 + 94.29i$. The optimization will focus on the state of the equivalent switch. It is clear in Fig. 5(b) that the number of buses decreases after the model is reduced, and the loop and structure are unchanged between the original network and the reduced network. Therefore, the solution space is reduced and optimal reconfiguration strategies can be obtained with fewer resources and less computation time.

C. Results of the IEEE 33-Bus Network

The database of the optimal reconfiguration strategy is built by the data-driven method based on the clustering model. According to the clustering results of the reduced network, the optimal reconfiguration strategies of potentially different load distributions can be separated into two clusters. The open switches of each loop are expressed in Table I.

According to the network recovery process, the two clusters can be recovered to a 19-bus network and an 18-bus network. An 18-bus network is displayed in Fig. 6, which is obtained by, respectively, adding the buses $(a_{21}, a_{22}, a_{23}, a_{24})$ in the branches (5′–6′, 6′–7′, 7′–8′, 3′–12′). Besides, the 19-bus network is obtained by adding the buses $(b_1, b_2, b_3, b_4, b_5)$ in the branches $(3'–4', 5'–6', 6'–7', 7'–8', 3'–12')$, respectively. The goal-oriented clustering model is used in two recovery networks to obtain the clusters, and the data-based LSTM learning network is used to build the database with the mapping mechanism, in which the database is for the second layer. Supposed 80% samples are the training samples, and the other 20% samples are the testing samples to test the training LSTM network. The LSTM learning is conducted in the MATLAB toolbox with 100% training accuracy. The reconfiguration strategy cluster of the 19-bus network and the 18-bus network are presented in Table II.

From Table II, it can be seen that in the second layer, there are identical reconfiguration strategies from different clusters of the first layer, i.e., the reconfiguration strategy $(4' - 9', 5' - b_2, b_3 - 7', b_4 - 8', b_5 - 12')$ is in both the 19-bus and 18-bus networks. This is a coupling phenomenon, which results from the layered recovery process. However, this coupling will not affect the accuracy of the reconfiguration strategy. For many paths from the reduced network to the original network during the recovery process, only one path needs to be in place.

From Fig. 6, the difference in the number of branches (i.e., switches) in each loop between the second layer network and the original network is not more than 2 ($N_0 = 2$ in this case). Therefore, the layered process ends, and the possible switch combinations after the layered process can be obtained. Then, the optimal reconfiguration strategy of the original network can be achieved by a simple selection process. The entire process is presented in Fig. 7.

According to the model reduction and recovery process, the optimal reconfiguration strategy of the first layer and the second layer can be expressed as $\{4' - 9', 5' - 6', 6' - 7', 7' - 8', 3' - 12'\}$ and $\{4' - 9', 5' - b_2, b_3 - 7', 7' - b_4, b_5 - 12'\}$ for load distribution, as shown in Fig. 8. There are four kinds of switch combinations after the layered process and corresponding minimum power losses can be calculated by the model (21) and (22), which are shown in Table III. Therefore, the optimal reconfiguration strategy of the original network is $\{4' - 9', 5' - b_2, c_2 - 7', 7' - b_4, c_3 - 12'\}$ and the power loss is 81.2806 kW.

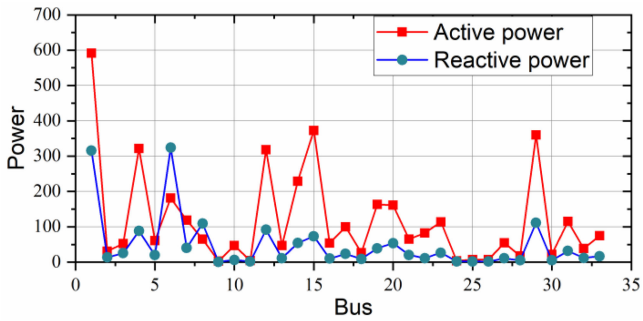

Fig. 8. Specific load distribution.

TABLE III
RECONFIGURATION STRATEGY AND POWER LOSSES

Cluster label	Loop 1	Loop 2	Loop 3	Loop 4	Loop 5	Power loss (kW)
1	4'-9'	5'-b_2	b_3-c_2	7'-b_4	b_5-c_3	86.9231
2	4'-9'	5'-b_2	b_3-c_2	7'-b_4	c_3-12'	86.8468
3	4'-9'	5'-b_2	c_2-7'	7'-b_4	b_5-c_3	81.5336
4	4'-9'	5'-b_2	c_2-7'	7'-b_4	c_3-12'	81.2806

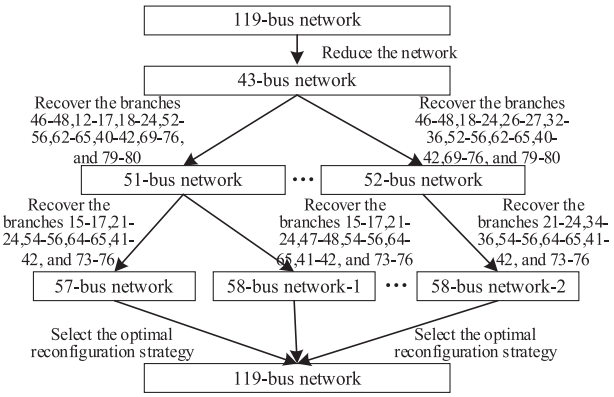

Fig. 9. Changing process of network.

D. Results of the IEEE 119-Bus Network

The IEEE 119-bus network [18] is used to show the effectiveness of the proposed HDNR framework in a large-scale network. It is noted that the index of switch combination is the same as the standard network that shows in the reference. For the IEEE 119-bus network, according to the model reduction, the reduced network is the 43-bus network. The database of the optimal reconfiguration strategy for the reduced network is built by the data-driven method, then conduct the hierarchical recovery process. As Fig. 9 shows, the first layer includes two major recovery networks: 51-bus network and 52-bus network. The second layer includes the 57-bus network and the 58-bus network (58-bus-1) corresponding to the 51-bus network in the first layer, and another 58-bus network (58-bus-2) corresponding to a 52-bus network in the first layer. The reconfiguration strategy clusters of these reduced networks are shown in Table IV. After two layers recovery, the remaining number of switch combinations in the 57-bus and 58-bus-2 network is 576, and that in 58-bus-1 is 1152. The optimal reconfiguration strategy of the original network can be obtained by directly judging these switch combinations based on (21) and (22).

TABLE IV
RECONFIGURATION STRATEGY OF REDUCED NETWORK

Network	Cluster label	Reconfiguration strategy
43-bus network	1	45-48, 11-17, 11-24, 51-56, 56-65, 61-65, 30-42, 95-100, 68-76, 78-91, 78-80, 86-113, 89-110, 115-123, 25-36
	2	45-48, 25-27, 11-24, 51-56, 56-65, 61-65, 30-42, 95-100, 68-76, 78-91, 78-80, 86-113, 89-110, 115-123, 31-36
51-bus network	1	45-46, 14-17, 20-24, 53-56, 56-65, 63-65, 40-42, 95-100, 72-76, 78-91, 79-80, 86-113, 89-110, 115-123, 25-36
	2	46-48, 14-17, 20-24, 53-56, 56-65, 63-65, 40-42, 95-100, 72-76, 78-91, 79-80, 86-113, 89-110, 115-123, 25-36
52-bus network	1	45-46, 26-27, 20-24, 53-56, 56-65, 63-65, 40-42, 95-100, 72-76, 78-91, 79-80, 86-113, 89-110, 115-123, 33-36

TABLE V
RECONFIGURATION STRATEGY OF REDUCED NETWORK FROM 123-BUS

Cluster label	Reconfiguration strategy				
	13-152	60-160	18-135 151-300	97-197	54-94
1	close	close	open	close	open
2	close	close	close	open	open

E. Results of the IEEE 123-Bus Network

For the IEEE 123-bus network [38], although there are 127 branches in the network, only 6 branches equip the switches, including 4 sectionalizing switches and 2 tie switches. Therefore, the network can be regarded as a 6-bus network through aggregating the nodal load next to the branch without switches to the bus next to the branch with switches. Then, the 5-bus network is obtained by model reduction. Table V shows the reconfiguration strategy of the 5-bus network. The reconfiguration database is built by the data-driven method. Because of the fewer switches, the original network can be directly obtained through recovering the 5-bus network. Then, the optimal reconfiguration strategy can be obtained through the (21) and (22).

F. Comparison Between the HDNR Framework and Different Methods

To show the effectiveness of the proposed HDNR framework in terms of computation time and optimal results, the comparison is conducted in the IEEE 33-bus, IEEE 119-bus, and IEEE 123-bus network. For the IEEE 33-bus network, the comparison methods include HSA, GA [19], SOE [15], and PSO [14], and the comparison results are shown in Table VI. Compared to HDNR, HSA, GA, PSO, and SOE are similar model-driven methods. In terms of power loss, the HDNR framework is the same as the HSA because of the similar calculation process, they both have the lowest value of 81.28 kW compared to GA, PSO, and SOE. The results of HDNR and HSA also show the model reduction and hierarchical recovery process proposed in this article will not affect the optimality of the reconfiguration results. In

TABLE VI
COMPARISON RESULTS OF THE IEEE 33-BUS NETWORK

Method	HDNR	HSA	GA	SOE	PSO
Strategy	4'-9', 5'-b_2, c_2-7', 7'-b_4, c_3-12'	4'-9', 5'-b_2, c_2-7', 7'-b_4, c_3-12'	1'-d_1,4'-5', b_2-c_1,7'-b_4, c_3-12'	4'-9', c_1-6', 7'-b_4, 12'-d_3, 3'-d_2	4'-9', 5'-b_2, c_2-7', 8'-13, d_2-b_5
Loss (kW)	81.28	81.28	151.25	100.50	112.21
Time (s)	0.09	7.20	8.38	1.00	10.64

TABLE VII
COMPARISON RESULTS OF THE IEEE 119-BUS NETWORK

Method	HDNR	HSA	GA	SOE
Strategy	45-46, 16-17, 22-23, 54-55, 56-65, 63-64, 41-42, 95-100, 74-75, 78-91, 79-80, 86-113, 89-110, 115-123, 25-36	45-46, 16-17, 22-23, 54-55, 56-65, 63-64, 41-42, 95-100, 74-75, 78-91, 79-80, 86-113, 89-110, 115-123, 25-36	46-47, 26-27, 8-24, 52-53, 62-63, 38-65, 41-42, 59-60, 75-76, 77-78, 100-101, 85-86, 89-110, 114-115, 24-25	45-46, 16-17, 22-23, 54-55, 56-65, 63-64, 41-42, 95-100, 74-75, 78-91, 79-80, 86-113, 89-110, 115-123, 25-36
Loss (kW)	305.02	305.02	331.94	305.02
Time (s)	23.65	196.19	103.36	96.64

TABLE VIII
COMPARISON RESULTS OF THE IEE 123-BUS NETWORK

Method	HDNR	HSA	GA	SOE
Strategy	151-300, 54-94	151-300, 54-94	151-300, 54-94	13-152, 54-94
Loss (kW)	220.50	220.50	220.50	456.12
Time (s)	0.02	2.66	11.40	2.64

terms of computation time, the HDNR is 0.09 s, which is far below the HSA, GA, PSO, SOE, and provides the possibility of real-time calculation. From the computation time and power losses, methods with the advantages of computation time may compromise computational accuracy, similar to that of SOE. However, they work together hierarchically in the proposed HDNR framework because the data-driven method is introduced to the reconfiguration model, getting the best performance in terms of both power loss and computation time.

For the IEEE 119-bus network, the comparison results are shown in Table VII with the methods: HSA, GA, and SOE. From Table VII, HSA, SOE, and the HDNR framework can get the same optimal reconfiguration strategy with the same minimum power loss, which is better than GA. Meanwhile, the computation time of the HDNR framework is the shortest, which is almost four times faster than the SOE. It is noted that the computation time of the HDNR framework is increased when compared with the IEEE 33-bus network, the reason is that the undetermined switch N_0 increases with the number of switches.

For the IEEE 123-bus network, the comparison is also conducted with the same methods of the IEEE 119-bus network. Table VIII shows the comparison results. The HDNR, HSA, and GA have the same optimal reconfiguration strategy and acquire the same minimum power loss, which is better than the SOE. The computation time of HDNR framework is also largely shorter than the other three methods.

Based on the comparison of the IEEE 33-bus, IEEE 119-bus, and IEEE 123-bus network, the proposed HDNR framework is efficient in both small-scale and large-scale networks with less online computation time and minimum power loss.

TABLE IX
COMPUTATION TIME OF EACH DATABASE

	Offline database		
IEEE 33-bus network	14-bus Samples 665	18-bus Samples 196	19-bus Samples 461
	34267 s	11246 s	27765 s
IEEE 119-bus network	43-bus Samples 665	51-bus Samples 140	52-bus Samples 142
	119770s	37808 s	42633 s
IEEE 123-bus network	5-bus Samples 665		
	127.47 s		

G. Analysis of Computation Cost and Practical Feasibility

The HDNR framework is implemented by using a computer with Intel Core i5-8250 CPU 1.60 GHz, 16 G memory, and MATLAB 2018a is used as the testing environment for the algorithm. The time for building each offline database is shown in Table IX. The time for building the database will increase with the bus number and sample number, where the bus number is the main influence factor (the time of building database in the IEEE 119-bus network is much longer than that in the IEEE 33-bus network). Although a certain time and computational resources are required to build the database, it is only recalculated when the network structure is changed, i.e., the scale of the system, which does not happen frequently when the load reaches saturation with the DN development. In practical applications, the database is built based on a long-term process with the offline operation, which only occupies the offline computational resources and has no effect on the online computation of obtaining optimal strategy. Therefore, these computation time and resources can be acceptable for the DNR problem. Besides, to further save the computational resources, the data samples can be dynamically added to the database. Considering that the database is built layer by layer, the database in the same layer can be built in a distributed way to save computation time. Moreover, the computation time can be further reduced when taking the solution tool with high performance (e.g., server) in the practical application.

In terms of the online computation time, it remains in the second level, as the results of the IEEE 119-bus network shown in Table VII. The online computation time is affected by the trained LSTM network and the undetermined switch N_0. The large-scale network may increase the input feature of the LSTM network, while the influence is slight. There will not be too many switch combinations because the number can be controlled by the hierarchical recovery process, and the calculation is fast since it only requires plugging the number in the formula.

For the IEEE 33-bus network, the accuracy of the LSTM network in the first layer is 95%, and the accuracy of the LSTM

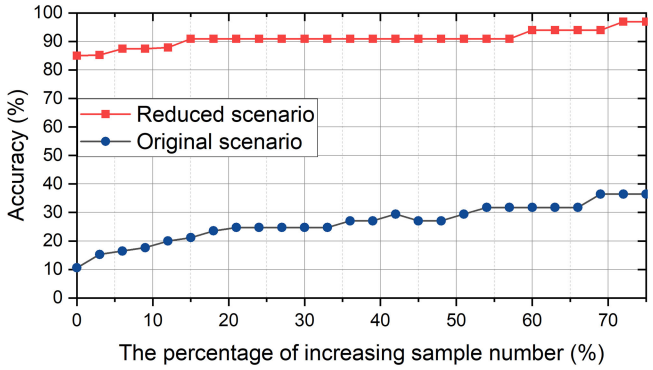

Fig. 10. Accuracy vs. number of samples.

networks corresponding to 18-bus and 19-bus networks in the second layer is 85% and 86%. For the IEEE 119-bus network, the accuracy of the LSTM network corresponding to 43-bus, and 51-bus networks are respective 96.36% and 91.67%. For the 5-bus network got by the IEEE 123-bus network, the accuracy is 93.47%. Because the samples should be separated into different categories as the hierarchical process occurs, reducing both the number of samples and the accuracy in the posterior layers. Besides, the learning accuracy of the reduced framework is higher than the original network, take the IEEE 33-bus network for example, the correlation between the accuracy and the increment of sample numbers is shown in Fig. 10. The reason is that the reduced scenario can reduce the solution space and the number of clusters. The accuracy will also increase with the increment of sample numbers in both the reduced and original scenarios, in which the data samples can be dynamically added to the framework in practical application.

VII. Conclusion

In this article, an HDNR framework was proposed, where the model reduction and goal-oriented clustering model were provided to obtain the data for a data-driven method. Furthermore, the LSTM network was suggested to learn the mapping mechanism for the reconfiguration strategy. The case study was conducted in the IEEE 33-bus, IEEE 119-bus, and IEEE 123-bus network. The number of buses in the DN was reduced by the model reduction, and the solution space was reduced correspondingly. The hierarchical database for the reduced networks was built by combining the network recovery process and the LSTM neural network. When compared with HSA, GA, PSO, and SOE, the HDNR method consumed less computation time and maintained minimum power losses in both small-scale and large-scale networks. Future studies will relate to new network reduction methods that simplify the network processing and explore the method to uncouple the DN for the distributed reconfiguration.

References

[1] L. Chen, N. Liu, and J. Wang, "Peer-to-peer energy sharing in distribution networks with multiple sharing regions," *IEEE Trans. Ind. Informat.*, vol. 16, no. 11, pp. 6760–6771, Nov. 2020.

[2] Y. Takenobu, N. Yasuda, S. Kawano, S. Minato, and Y. Hayashi, "Evaluation of annual energy loss reduction based on reconfiguration scheduling," *IEEE Trans. Smart Grid*, vol. 9, no. 3, pp. 1986–1996, May 2018.

[3] M. E. Baran and F. F. Wu, "Network reconfiguration in distribution systems for loss reduction and load balancing," *IEEE Trans. Power Del.*, vol. 4, no. 2, pp. 1401–1407, Apr. 1989.

[4] S. D. Kermany, M. Joorabian, S. Deilami, and M. A. S. Masoum, "Hybrid islanding detection in microgrid with multiple connection points to smart grids using fuzzy-neural network," *IEEE Trans. Power Syst.*, vol. 32, no. 4, pp. 2640–2651, Mar. 2017.

[5] R. A. Jabr, R. Singh, and B. C. Pal, "Minimum loss network reconfiguration using mixed-integer convex programming," *IEEE Trans. Power Syst.*, vol. 27, no. 2, pp. 1106–1115, May 2012.

[6] C. Lee, C. Liu, S. Mehrotra, and Z. Bie, "Robust distribution network reconfiguration," *IEEE Trans. Smart Grid*, vol. 6, no. 2, pp. 836–842, Mar. 2015.

[7] M. R. Dorostkar-Ghamsari, M. Fotuhi-Firuzabad, M. Lehtonen, and A. Safdarian, "Value of distribution network reconfiguration in presence of renewable energy resources," *IEEE Trans. Power Syst.*, vol. 31, no. 3, pp. 1879–1888, May 2016.

[8] Y. Song, Y. Zheng, T. Liu, S. Lei, and D. J. Hill, "A new formulation of distribution network reconfiguration for reducing the voltage volatility induced by distributed generation," *IEEE Trans. Power Syst.*, vol. 35, no. 1, pp. 496–507, Jan. 2020.

[9] A. Hamidi, S. Golshannavaz, and D. Nazarpour, "D-FACTS cooperation in renewable integrated microgrids: A linear multiobjective approach," *IEEE Trans. Sustain. Energy*, vol. 10, no. 1, pp. 355–363, Jan. 2019.

[10] C. Wang, S. Lei, P. Ju, C. Chen, C. Peng, and Y. Hou, "MDP-based distribution network reconfiguration with renewable distributed generation: Approximate dynamic programming approach," *IEEE Trans. Smart Grid*, vol. 11, no. 4, pp. 3620–3631, Jul. 2020.

[11] J. A. Taylor and F. S. Hover, "Convex models of distribution system reconfiguration," *IEEE Trans. Power Syst.*, vol. 27, no. 3, pp. 1407–1413, Aug. 2012.

[12] R. S. Rao, S. V. L. Narasimham, M. R. Raju, and A. S. Rao, "Optimal network reconfiguration of large-scale distribution system using harmony search algorithm," *IEEE Trans. Power Syst.*, vol. 26, no. 3, pp. 1080–1088, Aug. 2011.

[13] R. S. Rao, K. Ravindra, K. Satish, and S. V. L. Narasimham, "Power loss minimization in distribution system using network reconfiguration in the presence of distributed generation," *IEEE Trans. Power Syst.*, vol. 28, no. 1, pp. 317–325, Feb. 2013.

[14] S. Chen, W. Hu, and Z. Chen, "Comprehensive cost minimization in distribution networks using segmented-time feeder reconfiguration and reactive power control of distributed generators," *IEEE Trans. Power Syst.*, vol. 31, no. 2, pp. 983–993, Mar. 2016.

[15] J. Zhan, W. Liu, C. Y. Chung, and J. Yang, "Switch opening and exchange method for stochastic distribution network reconfiguration," *IEEE Trans. Smart Grid*, vol. 11, no. 4, pp. 2995–3007, Jul. 2020.

[16] S. Mishra, D. Das, and S. Paul, "A comprehensive review on power distribution network reconfiguration," *Energy Syst.*, vol. 8, no. 2, pp. 227–284, Mar. 2017.

[17] A. Mendes, N. Boland, P. Guiney, and C. Riveros, "Switch and tap-changer reconfiguration of distribution networks using evolutionary algorithms," *IEEE Trans. Power Syst.*, vol. 28, no. 1, pp. 85–92, Feb. 2013.

[18] D. Zhang, Z. Fu, and L. Zhang, "An improved TS algorithm for loss-minimum reconfiguration in large-scale distribution systems," *Elect. Power Syst. Res.*, vol. 77, no. 5/6, pp. 685–694. Apr. 2007.

[19] S. Golshannavaz, S. Afsharnia, and F. Aminifar, "Smart distribution grid: Optimal day-ahead scheduling with reconfigurable topology," *IEEE Trans. Smart Grid*, vol. 5, no. 5, pp. 2402–2411, Sep. 2014.

[20] A. M. R. Antonio, B. R. Anselmo, and M. G. Silva, "Robust meter placement for state estimation considering distribution network reconfiguration for annual energy loss reduction," *Elect. Power Syst. Res.*, vol. 182, 2020, Art. no. 106233.

[21] C. Peng, L. Xu, X. Gong, H. Sun, and L. Pan, "Molecular evolution based dynamic reconfiguration of distribution networks with DGs considering three-phase balance and switching times," *IEEE Trans. Ind. Informat.*, vol. 15, no. 4, pp. 1866–1876, Apr. 2019.

[22] A. Ali, N. Hossein, N. Ehsan, F. Mehdi, and R. N. Mohammad, "A hybrid evolutionary algorithm for secure multi-objective distribution feeder reconfiguration," *Energy*, vol. 138, pp. 355–373, 2017.

[23] T. Ding, Q. Yang, Y. Yang, C. Li, Z. Bie, and F. Blaabjerg, "A data-driven stochastic reactive power optimization considering uncertainties in active distribution networks and decomposition method," *IEEE Trans. Smart Grid*, vol. 9, no. 5, pp. 4994–5004, Sep. 2018.

[24] A. S. Zamzam, X. Fu, and N. D. Sidiropoulos, "Data-driven learning-based optimization for distribution system state estimation," *IEEE Trans. Power Syst.*, vol. 34, no. 6, pp. 4796–4805, Nov. 2019.
[25] J. Yu, Y. Weng, and R. Rajagopal, "PaToPa: A data-driven parameter and topology joint estimation framework in distribution grids," *IEEE Trans. Power Syst.*, vol. 33, no. 4, pp. 4335–4347, Jul. 2018.
[26] S. J. Pappu, N. Bhatt, R. Pasumarthy, and A. Rajeswaran, "Identifying topology of low voltage distribution networks based on smart meter data," *IEEE Trans. Smart Grid*, vol. 9, no. 5, pp. 5113–5122, Sep. 2018.
[27] Y. Zhou, R. Arghandeh, and C. J. Spanos, "Partial knowledge data-driven event detection for power distribution networks," *IEEE Trans. Smart Grid*, vol. 9, no. 5, pp. 5152–5162, Sep. 2018.
[28] A. Akrami, M. Doostizadeh, and F. Aminifar, "Optimal reconfiguration of distribution network using μPMU measurements: A data-driven stochastic robust optimization," *IEEE Trans. Smart Grid*, vol. 11, no. 1, pp. 420–428, Jan. 2020.
[29] Y. Gao, W. Wang, J. Shi, and N. Yu, "Batch-constrained reinforcement learning for dynamic distribution network reconfiguration," *IEEE Trans. Smart Grid*, vol. 11, no. 6, pp. 5357–5369, Nov. 2020.
[30] X. Ji, Z. Yin, Y. Zhang, B. Xu, and Q. Liu, "Real-time autonomous dynamic reconfiguration based on deep learning algorithm for distribution network," *Elect. Power Syst. Res.*, vol. 195, 2021, Art. no. 107132.
[31] B. Enacheanu, B. Raison, R. Caire, O. Devaux, W. Bienia, and N. HadjSaid, "Radial network reconfiguration using genetic algorithm based on the matroid theory," *IEEE Trans. Power Syst.*, vol. 23, no. 1, pp. 186–195, Feb. 2008.
[32] N. Biggs, E. Lloyd, and R. Wilson, *Graph Theory*. London, U.K.: Oxford Univ. Press, 1986, pp. 1736–1936.
[33] T. L. Baldwin, L. Mili, and A. G. Phadke, "Dynamic ward equivalents for transient stability analysis," *IEEE Trans. Power Syst.*, vol. 9, no. 1, pp. 59–67, Feb. 1994.
[34] C. Ababei and R. Kavasseri, "Efficient network reconfiguration using minimum cost maximum flow-based branch exchanges and random walks-based loss estimations," *IEEE Trans. Power Syst.*, vol. 26, no. 1, pp. 30–37, Feb. 2011.
[35] A. Al-Wakeel, J. Wu, and N. Jenkins, "K-means based load estimation of domestic smart meter measurements," *Appl. Energy*, vol. 194, pp. 333–342, May 2017.
[36] K. Nekooei, M. M. Farsangi, H. Nezamabadi-Pour, and K. Y. Lee, "An improved multi-objective harmony search for optimal placement of DGs in distribution systems," *IEEE Trans. Smart Grid*, vol. 4, no. 1, pp. 557–567, Mar. 2013.
[37] I. Goodfellow, Y. Bengio, and A. Courville, "Sequence modeling: Recurrent and recursive nets," in *Deep Learning*. Cambridge, MA, USA: MIT Press, 2016.
[38] W. H. Kersting, "Radial distribution test feeders," *IEEE Trans. Power Syst.*, vol. 6, no. 3, pp. 975–985, Aug. 1991.

Nian Liu (Member, IEEE) received the B.S. and M.S. degrees from Xiangtan University, Hunan, China, in 2003 and 2006, respectively, and the Ph.D. degree from North China Electric Power University, Beijing, China, in 2009, all in electrical engineering.

He is currently a Professor and the Vice Dean with the School of Electrical and Electronic Engineering, North China Electric Power University. He is also the Director of Research Section for Multi-information Fusion and Integrated Energy System Optimization with the State Key Laboratory of Alternate Electrical Power System with Renewable Energy Sources, Beijing. From 2015 to 2016, he was a Visiting Research Fellow with the Royal Melbourne Institute of Technology University (RMIT), Melbourne, Australia. He has authored or coauthored more than 180 journal and conference publications and has been granted more than 20 patents of China. His major research interests include multienergy system integration, microgrids, cyber-physical energy system, and renewable energy integration.

Dr. Liu is a Member of the Standardization Committee of Power Supply and Consumption in the Power Industry of China. He was the Highly Cited Chinese Researcher of Elsevier in 2020. He is the Editor of the IEEE TRANSACTIONS ON SMART GRID, IEEE TRANSACTIONS ON SUSTAINABLE ENERGY, IEEE Power Engineering Letters, and *Journal of Modern Power Systems and Clean Energy (MPCE)*.

Chenchen Li (Student Member, IEEE) is currently working toward the master's degree in electrical engineering with the School of Electrical and Electronic Engineering, North China Electric Power University, Beijing, China.

Her research interests include energy management and demand response in distribution system and distribution network reconfiguration.

Liudong Chen (Student Member, IEEE) is currently working toward the master's degree in electrical engineering with the School of Electrical and Electronic Engineering, North China Electric Power University, Beijing, China.

His research interests include energy management, smart grids, and optimization theory and its application in distribution system.

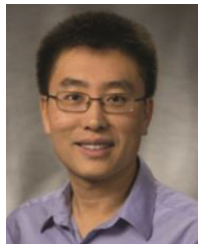

Jianhui Wang (Fellow, IEEE) received the Ph.D. degree in electrical engineering from the Illinois Institute of Technology, Chicago, IL, USA, in 2007.

He is currently a Professor with the Department of Electrical and Computer Engineering, Southern Methodist University, Dallas, TX, USA. He has authored and/or coauthored more than 300 journal and conference publications, which have been cited for more than 30000 times by his peers with an H-index of 87. He has been invited to give tutorials and keynote speeches at major conferences including IEEE ISGT, IEEE SmartGridComm, IEEE SEGE, IEEE HPSC, and IGEC-XI.

Dr. Wang is the past Editor-in-Chief of the IEEE TRANSACTIONS ON SMART GRID and an IEEE PES DISTINGUISHED LECTURER. He is also a Guest Editor for the Special Issue on Power Grid Resilience of the Proceedings of the IEEE. He was the recipient of the IEEE PES POWER SYSTEM OPERATION COMMITTEE Prize Paper Award in 2015, the 2018 Premium Award for Best Paper in *IET Cyber-Physical Systems: Theory and Applications*, the Best Paper Award in the IEEE TRANSACTIONS ON POWER SYSTEMS in 2020, and the IEEE PES Power System Operation, Planning and Economics Committee Prize Paper Award in 2021. He is a Clarivate Analytics Highly Cited Researcher for the production of multiple highly cited papers that rank in the top 1% by citations for field and year in Web of Science (2018–2020).